New method for equation-of-state calculations: Linear combinations of basis potentials

Yaakov Rosenfeld

Nuclear Research Center-Negev, P. O. Box 9001, Beer Sheva, Israel

(Received 12 November 1981)

A new method presented here for calculating the equation of state for classical systems is very fast, employs the same algorithm for all solid and fluid densities and temperatures, and is of accuracy comparable with that of the computer simulations. The method consists of fitting the pair potential by a linear combination of potentials belonging to a basis set (for which the inverse power potentials are a good choice) and of employing a property of additivity of equations of state when these are considered in terms of the density and excess entropy as the independent variables. The new method accomodates the static lattice sum, or any physical quantity that is expected to be additive in pair-potential contributions, as naturally as the pair potential itself, and should be very useful in the study of equations of state for real materials. There are indications for the validity of the new method in two dimensions as well.

I. INTRODUCTION

A theory for the thermodynamic properties of classical systems of particles, with given pair-interaction potentials, that is accurate, fast in calculations, and that employs the same algorithm over the full range of solid and fluid densities, is a basic and important tool is studying equations of state for real materials. Computer simulations are accurate but not fast enough to provide the needed flexibility when adjusting the classical potential to the experimental data. That needed flexibility is obtained by reducing the accuracy: cell theory, lattice dynamics in the harmonic approximation, or their Grüneisen-type simplifications, are the "standard" theories for classical solids,[1] while perturbation theories, with the hard spheres as the virtually unanimous choice for the reference system, serve an equally important role for fluids.[2] These (first-order) theories are usually accurate to no better than 5% in the excess free energy near the solid-fluid transition. There have been attempts[3,4] recently to modify these theories such thay they employ the zero-temperature isotherm (i.e., the static lattice sum of the classical effective pair potential) directly, instead of the pair potential itself.

Here we present a new method for calculating the equation of state (EOS) for classical systems, with given spherically symmetric pair interactions, which is very fast in calculations, employs the same algorithm for all densities and temperatures, and with accuracy comparable with that obtained by standard computer simulations (overall accuracy better than 2%). This new method accomodates the static lattice sum or any physical quantity that is expected to be additive in pair interactions, as naturally as the pair potential itself. If the solid is treated in the harmonic approximation, the new method is equivalent to an improved version of the Grüneisen theory.

The paper is organized as follows: In Sec. II we introduce a "variational fitting procedure" for fitting EOS data, and show that the computer-simulation results for a wide variety of potentials that are relatively soft (i.e., do not contain a hard core) can be thus fitted by a universal set of fitting functions. In Sec. III a useful statement that follows from the above universality is derived. If a given potential is a linear combination of other potentials and if we choose the density and excess entropy as the independent thermodynamic variables, then the EOS for the given potential is expressed in terms of those for the other potentials in a simple additive manner. The inverse power potentials are considered as a "basis set" for EOS calculations. A benchmark test of the accuracy of the new method, via the EOS for the Lennard-Jones fluid, is given in Sec. IV. Simple classical solids and improvements upon the standard Grüneisen theory are discussed in Sec. V, while additive melting equations that describe the fluid-solid transition are derived in Sec. VI. Finally, Sec. VII contains a brief summary and the main conclusions.

II. VARIATIONAL FITTING PROCEDURE AND UNIVERSALITY OF THE FITTING FUNCTIONS

Consider a classical system of particles interacting through a spherically symmetric (and possibly density-dependent) pair potential, $\phi(r;\rho)$, for which the EOS is known: $S^E/Nk_B = s_\phi(\rho,T), U/N = u_\phi(\rho,T)$, where S^E and U are, respectively, the excess entropy and potential energy of the system as functions of the density ρ and temperature T. Let $S_{0,\phi}(\rho,\mu)$ and $g_{0,\phi}(s;\rho,\mu)$ be one parameter (i.e., μ) functions by which the given EOS is fitted according to the following "variational fitting procedure" (VFP):

$$s_\phi(\rho,T) \cong s_{0,\phi}(\rho,\mu) , \tag{1}$$

$$U_\phi(\rho,T) \cong U_{0,\phi}(\rho,\mu) \equiv \tfrac{1}{2}\rho \int g_{0,\phi}(r;\rho,\mu)\phi(r;\rho)d\vec{r} , \tag{2}$$

$$\frac{\partial}{\partial\mu}[-Ts_{0,\phi}(\rho,\mu) + U_{0,\phi}(\rho,\mu)]|_{\rho,T} = 0 . \tag{3}$$

Equation (3), by which μ is determined as function of ρ and T, is a requirement of thermodynamic consistency. It results from imposing the usual thermodynamic relation, $s = -(\partial f/\partial T)_\rho$, on the approximate (fitting) excess free energy per particle,

$$f_{0,\phi}(\rho,\mu,T) = -Ts_{0,\phi}(\rho,\mu) + U_{0,\phi}(\rho,\mu) ,$$

and the excess entropy per particle, $s_{0,\phi}(\rho,\mu)$. If the fitting function $s_{0,\phi}(\rho,\mu)$ is the excess entropy of some (reference) system, and $g_{0,\phi}(r;\rho,\mu)$ is the corresponding radial distribution function, then VFP becomes identical to the variational form of first-order perturbation theory based on the Gibbs-Bogoliubov inequality.[5]

The new approach to EOS calculations that is introduced in the present work is based on the premise that it is possible to obtain VFP fits for the EOS of quite disparate potentials with accuracy of the order of, or slightly worse than, the accuracy of the Monte Carlo (MC) results by the same (universal) fitting functions, independent of the pair potential,

$$s_{0,\phi}(\rho,\mu) = s_0(\rho,\mu) , \tag{4a}$$

$$g_{0,\phi}(\rho,\mu) = g_0(\rho,\mu) , \tag{4b}$$

with possibly different universal functions s_0, g_0, for the fluid and solid phase. The possibility of such one-parameter scaling of the configurational phase space for simple systems is deduced from

numerous applications of first-order perturbation theories (in their variational mode) to a wide variety of systems and, as a matter of fact, it is the reason underlying their success.

A. Fluid

The hard-sphere (HS) approach to perturbation theory for fluids, based on the Gibbs-Bogoliubov inequality with the hard spheres as the reference system, proved successful for many types of potentials.[6] Most of the variational HS calculations were performed with the Carnahan-Starling[7] (CS) expression for the HS excess entropy and the Percus-Yevick[8] (PY) result for the radial distribution function, amounting to the following universal fitting functions in the VFP.

$$s_0(\rho,\mu) = s_{CS}(\eta) = -\frac{4\eta - 3\eta^2}{(1-\eta)^2} , \tag{5a}$$

$$g_0(r;\rho,\mu) = g_{PY}(r/d;\eta) , \tag{5b}$$

where d is the HS diameter, and $\eta = (\pi/6)\rho d^3$ is the HS packing fraction. It has been observed[9,10] that an *ad hoc* correction to $s_{CS}(\eta)$, namely, $s_0(\eta) = s_{CS}(\eta) + \eta$, while keeping (5b), leads to a general improvement of the prediction of the theory for a wide range of potentials (e.g., 2% agreement with simulations for the r^{-6}, r^{-9}, r^{-12}, exp-6, and screened Coulomb potentials). Ross has recently suggested[11] a "bootstrap" approach in which: (a) the known EOS for some reference potential is fitted as accurately as possible by the VFP using (5b) but with an *ad hoc* correction to (5a), $s_0(\eta) = s_{CS}(\eta) + \delta s_0(\eta)$: and (b) the same fitting functions are employed in the VFP to obtain the EOS for another potential. By applying that bootstrap approach, Ross found that the function

$$s_0(\eta) = s_{CS}(\eta) + \left[\frac{\eta}{2} + \eta^2 + \frac{\eta^4}{4}\right] ,$$

chosen to reproduce the MC EOS for the r^{-12} potential, gives results for the r^{-6}, r^{-9}, Lennard-Jones (12-6), and exp-6 potentials to an accuracy of about 2% or less. Furthermore, the choice

$$s_o(\eta) = -\frac{6\eta}{1-\eta} - 2\ln(1-\eta) .$$

i.e., the PY virial hard-sphere EOS, reproduces by the VFP the analytic form suggested by De Witt[12] for the asymptotic (strong-coupling) fluid EOS for the inverse power potentials.[13] Although a particular choice for $\delta s_0(\eta) = \delta s_0^{(1)}(\eta)$ that fits particular-

ly well the simulation data for one type of potentials (say, relatively hard) may be somewhat worse than another choice, $\delta s_0(\eta) = \delta s_0^{(2)}(\eta)$, when fitting another type (say, relatively soft), all these results indicate that a universal function $\delta s_0(\eta)$ can be found that will produce 2% accurate VFP fits for any kind of potential) in the dense-fluid regime, provided it does not have a hard core. In view of the yet untried additional freedom to change $g_0(r/d;\eta)$, we expect the premise of universality of the fitting functions to have the accuracy of the present-day simulation studies for dense simple classical fluids.

B. Solid

The variational approach with the spherically averaged harmonic cell model as the reference system gives good results for the EOS of simple solids, i.e., with accuracy comparable with that of the HS theory for dense liquids.[5] The first-order choice for a universal VFP fitting functions [the "solid" counterparts of (5a) and (5b)] will be[4]

$$s_0(\rho,A) = -\ln\rho - \tfrac{3}{2}\ln A + C \ , \tag{6a}$$

$$g_0(r,\rho,A) = \frac{1}{\rho}\sum_l \frac{n_l}{a_l^3} \left[\frac{Aa_l^2}{4\pi a_1^2}\right]^{1/2} \frac{1}{4\pi(r/a_l)}$$

$$\times \exp\left[-\frac{Aa_l^2}{4a_1^2}\left[\frac{r}{a_l}-1\right]^2\right] \ , \tag{6b}$$

where C is a universal constant, n_l and a_l are the number and position of the lth nearest neighbors of a given particle on the lattice, $a_1 = (\gamma_0\rho)^{-1/3}$ where γ_0 depends on the lattice structure ($r_0 = 1/\sqrt{2}$ for fcc), and A is the force constant related to the Lindeman parameter δ by $A = 3/\delta^2$. The VFP with (6a) and (6b) leads to a Grüneisen-type description of the simple solid EOS. In particular, a simplified form of (6b), namely,[4]

$$g_0(r;\rho,A) = \frac{1}{\rho}\sum_l \frac{n_l}{a_l^3}\left[\frac{A}{4\pi}\right]^{1/2}\frac{1}{4\pi(r/a_l)}$$

$$\times \exp\left[-\frac{A}{4}\left[\frac{r}{a_l}-1\right]^2\right] \tag{7}$$

when used in the VFP with (6a), leads to the Grüneisen EOS with the usual "free-volume"

Grüneisen parameter (see Sec. V A). *Ad hoc* modifications of (6a) and/or (6b) have not been tried, but it is expected that the configurational phase space of simple solids will obey one-parameter scaling at least as accurately as that for simple dense fluids (see Sec. V C).

III. ADDITIVE EQUATIONS OF STATE AND THE INVERSE POWER POTENTIALS AS THE BASIS SET

Universality of the VFP fitting functions means that equations of state for different potentials may have many common features provided we choose the density, ρ, and excess entropy, s, as the independent variables. In particular, a property of additivity, to be described below, has important practical implications.

Suppose that a given potential can be expressed as a linear combination of other potentials (with possibly density-dependent coefficients),

$$\phi(r;\rho) = \sum_i \alpha_i(\rho)\phi_1(r;\rho) \ . \tag{8}$$

To the extent that the VFP fitting functions are universal and accurate, i.e., that the approximate equalities (1), (2), (4a), and (4b) are true equalities for any potential of the set $\{\phi,\{\phi_i\}\}$, then μ becomes [via Eq. (1)] a universal function of the excess entropy s, leading [via Eq. (2)] to additivity of equations of state:

$$U_\phi^{(s)}(\rho,s) = \sum_i \alpha_i(\rho)U_{\phi_i}^{(s)}(\rho,s) \ , \tag{9}$$

where $U_{\phi_k}^{(s)}(\rho,s)$ is the function describing the potential energy per particle for the potential ϕ_k as function of ρ and s. Thus knowing the EOS for the potentials ϕ_i and choosing ρ and s as the independent variables, we can construct the EOS for any linear combination of these potentials.

Given accurate equation of state (from simulations or from modified HNC calculations[14]) for a set of potentials (the "basis set"), one may fit another potential by a linear combination of potentials belonging to the basis set and use Eq. (9) to construct the EOS for that potential. In the general mode of application the basis set could, in principle, be a set of materials for which the EOS is known experimentally and the linear combination can be composed of any physical quantity that is expected to be additive in potentials (the zero-temperature isotherm or static-lattice sum are such quantities).

The set of inverse power potentials, $\phi_n(r)$ $=\epsilon(\sigma/r)^n$, is a particularly useful basis set for the following main reasons: (i) A linear combination of inverse powers can fit well nearly any physically conceivable effective pair potential; and (ii) due to their homogeneity, the inverse power potentials have the scaling property that a single isotherm or isochore describes the complete EOS, i.e., the excess thermodynamics depends only on the reduced temperature-density variable $y_n=\rho^*/T^{*3/n}$, where $\rho^*=\rho\sigma^3$ and $T^*=k_BT/\epsilon$; (iii) accurate computer-simulation data[2,15-18] exist for $n=1,4,6,9,12,\infty$ to permit, by interpolation procedures, the construction of $U_n^{(s)}(\rho,s)$ for every power n.

The computer-simulation data is given in the form $\beta P/\rho-1=Z_n^{\text{ex}}(y_n)$ or

$$\beta\epsilon U_n(y_n)=\frac{3}{n}Z_n^{\text{ex}}(y_n) ,$$

where $\beta=(k_BT)^{-1}$. The excess entropy is obtained by

$$s=\frac{S^{\text{ex}}}{Nk_B}=\frac{3}{n}Z_n^{\text{ex}}(y_n)-\int_0^{y_n}\frac{Z_n^{\text{ex}}(x)}{x}dx ,$$

and this relation can be inverted to yield $y_n(s)$. Finally,

$$U_n^{(s)}(\rho^*,s)=\frac{3}{n}Z_n^{\text{ex}}(y_n)\left[\frac{\rho^*}{y_n(s)}\right]^{n/3}$$

$$\equiv U_n^0(s)\rho^{*n/3} .$$

The melting transition is characterized by the values $s_L^{(n)}$, $s_S^{(n)}$ on the liquid (L) and solid (S) side of the transition. The liquid and solid densities are given by (see Table I)

$$\rho_L^{*(n)}=y_n(s_L^{(n)})T_n^{*3/n} ,$$

$$\rho_S^{*(n)}=y_n(s_S^{(n)})T_n^{*3/n} ,$$

and the melting curve is

$$P_M^{*(n)}=[1+Z_n^{\text{ex}}(y_n(s_L^{(n)}))]y_n(s_L^{(n)})T_n^{*1+3/n}$$

$$=[1+Z_n^{\text{ex}}(y_n(s_S^{(n)}))]y_n(s_S^{(n)})T_n^{*1+3/n} ,$$

where $P^*=P\sigma^3/\epsilon$ is the reduced pressure and the index M denotes "melting." Given the combination

$$\phi(r;\rho)=\epsilon\sum_n\alpha_n(\rho)(\sigma/r)^n , \tag{10}$$

the additive EOS [Eq. (9)] yields

$$U^{(s)}(\rho,s)=\epsilon\sum_n\alpha_n(\rho)U_n^0(s)\rho^{*n/3} . \tag{11}$$

Equation (11) together with standard thermodynamic relations provide a complete EOS for the potential ϕ. A routine that is useful for constructing the EOS in table form once the tables

$$\{y_n(s^{(i)})=y_n^{(i)}, \ i=1,2,...,q\}$$

are given, is the following.

From the thermodynamic identity, $T=[\partial U^{(s)}(\rho,s)/\partial s]_\rho$, we obtain

$$T^*=\sum_n\alpha_n(\rho)\left[\frac{\rho^*}{y_n(s)}\right]^{n/3} . \tag{12}$$

Choose a particular isotherm T^* and solve Eq. (12) for $\rho^{*(i)}$ for any given $s^{(i)}$. Define $Y_n^{(i)}=\rho^{*(i)}/T^{*3/n}$. Let O stand for either U/T^* or F^{ex}/Nk_BT (the excess free energy) and let O_n be the corresponding quantity for the inverse nth power potential. From Eqs. (11) and (12) we get

$$O(\rho^{*(i)},T^*)=\sum_n\alpha_nO_n(y_n^{(i)})\left[\frac{Y_n^{(i)}}{y_n^{(i)}}\right]^{n/3} . \tag{13}$$

Relation (13) also holds for $O=\beta P/\rho-1$ if the coefficients α_n are density independent. The melting characteristics for a given isotherm T^*, i.e., ρ_L, ρ_S, S_L, s_S are obtained by imposing thermal

$$\sum_n\alpha_n\left[\frac{\rho_S^*}{y_n(s_S)}\right]^{n/3}=\sum_n\alpha_n\left[\frac{\rho_L^*}{y_n(s_L)}\right]^{n/3}$$

$$=T^* , \tag{14a}$$

mechanical

$$\sum_n\alpha_n[1+Z_n^{\text{ex}}(y_n(s_L))]y_n(s_L)\left[\frac{\rho_L^*}{y_n(s_L)}\right]^{1+n/3}=\sum_n\alpha_n[1+Z_n^{\text{ex}}(y_n(s_S))]y_n(s_S)\left[\frac{\rho_S^*}{y_n(s_S)}\right]^{1+n/3} , \tag{14b}$$

and chemical equilibrium

TABLE I. Data for inverse power potentials. For the meaning of the various quantities, see the text.

n	C_n	D_n	$-s_L^{(n)}$	$-s_S^{(n)}$	$y_n(s_L^{(n)})/\sqrt{2}$	$y_n(s_S^{(n)})/\sqrt{2}$	$C_{\text{Einstein}}^{(n)}$	Δ_n	$C_{\text{LD}}^{(n)}$	$C_{\text{MC}}^{(n)}$
4	7.9811	18.2109	4.00	4.79	3.92	3.94	-1.789	0.513	-1.276	-1.354
6	3.6135	32.0045	3.68	4.42	1.54	1.56	-2.635	0.437	-2.198	-2.283
9	2.2084	51.7646	3.64	4.45	0.943	0.971	-3.356	0.374	-2.982	-3.024
12	1.5165	66.3243	3.85	4.71	0.814	0.844	-3.738	0.340	-3.398	-3.651

$$\sum_n \alpha_n \left[s_L + \frac{3}{n} Z_n^{\text{ex}}(y_n(s_L)) + \ln y_n(s_L) + \ln \frac{\rho_L^*}{y_n(s_L)} \right] \left[\frac{\rho_L^*}{y_n(s_L)} \right]^{n/3}$$

$$= \sum_n \alpha_n \left[s_S + \frac{3}{n} Z_n^{\text{ex}}(y_n(s_S)) + \ln y_n(s_S) + \ln \left[\frac{\rho_S^*}{y_n(s_S)} \right] \right] \left[\frac{\rho_S}{y_n(s_S)} \right]^{n/3} \quad (14\text{c})$$

between the liquid (L) and solid (S) phases.

IV. FLUID: THE LENNARD-JONES SYSTEM AS A BENCHMARK EXAMPLE

The equations of state for the state ($n \le 12$) inverse power fluids reveal various universal characteristics that enable accurate interpolations between existing computers-simulation data. In particular we mention the scaling via the Einstein frequency,[17] the universal form of the EOS in strong coupling,[12,13] and the facts that the entropy change across the melting transition, as well as the excess entropy on the liquid side of the transition, are nearly the same for all n.[17] Modified HNC calculations[14] aimed at extending the existing MC data for other powers n are underway.

During the course of fitting MC data we found a very simple and highly accurate fit for those cases for which $n/3 = m =$ integer:

$$Z_n^{\text{ex}}(y_n) = \sum_{i=1}^{m-1} B_i^{(n)} y_n^i + m C_n y_n^m + G y_n^{(m^2+m-1)/(m+1)} , \quad (15)$$

where the $B_i^{(n)}$'s are the exact first $m-1$ virial coefficients, $C_n y_n^m$ is the fcc static-lattice energy, and G is the only free parameter of the fit. We obtain

$$Z_6^{\text{ex}}(y) = 3.7124y - 0.9944y^{5/3} + 7.2270y^2 , \quad (16\text{a})$$

$$-s = 1.8562y - 0.09944y^{5/3} , \quad (16\text{b})$$

for $n = 6$,

$$Z_9^{\text{ex}}(y) = 2.8359y + 4.2756y^2 - 2.2999y^{2.75} + 6.6252y^3 , \quad (17\text{a})$$

$$-s = 1.8906y + 0.7126y^2 - 0.06973y^{2.75} , \quad (17\text{b})$$

for $n = 9$, and

$$Z_{12}^{\text{ex}}(y) = 2.5664y + 3.7908y^2 + 3.5282y^3 - 3.1508y^{3.8} + 6.0660y^4 , \quad (18\text{a})$$

$$-s = 1.9248y + 0.9477y^2 + 0.2940y^3 - 0.04155y^{3.8} , \quad (18\text{b})$$

for $n = 12$.

A benchmark test for the accuracy of the additive EOS [Eq. (9)] is provided by the Lennard-Jones (LJ) potential

$$\phi_{\text{LJ}}(r) = 4\epsilon \left[\left[\frac{\sigma}{r} \right]^{12} - \left[\frac{\sigma}{r} \right]^6 \right] . \quad (19)$$

Using the procedure outlined in Sec. III together with the EOS for the inverse 6 and 12 power potentials given by Eqs. (16) and (18) above, we obtain the results summarized in Figs. 1−3 and in Tables II−IV. Except for the region defined roughly by temperatures below the critical temperature ($T_{C,\text{LJ}}^* \simeq 1.36$) *and* densities below the critical density ($\rho_{C,\text{LJ}}^* \cong 0.36$), the additive EOS agrees with the MC data[2,18] for the LJ system to within their statistical error.[19]

V. SOLID

A. The standard Grüneisen theory

The Grüneisen EOS for solids is given by[20]

$$P(\rho, T) = P_0(\rho) + P_{\text{th}}(\rho, T) , \quad (20)$$
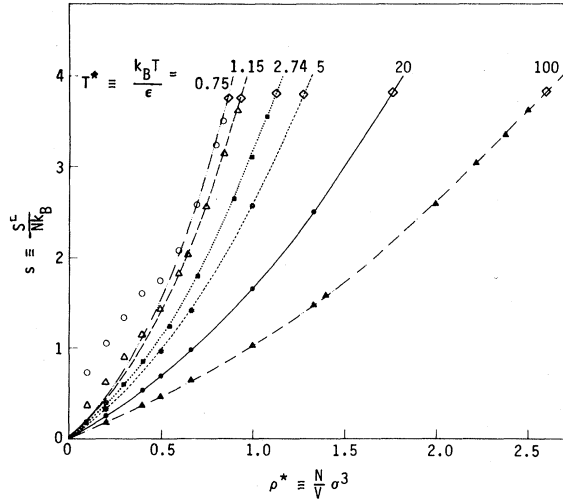
FIG. 1. Excess entropy as function of reduced density and reduced temperature for the Lennard-Jones fluid. The curves are the results of the present method and the points represent the Monte Carlo (Ref. 18) data. The diamond symbols represent the fluid side of the fluid-solid transition.

$$P_{\text{th}}(\rho,T)=\gamma_G(\rho)\rho E_{\text{th}}(\rho,T) , \qquad (21)$$

where $P_0(\rho)=\rho^2(\partial/\partial\rho)\,U_0(\rho)$ is the pressure at zero temperature (the "cold" pressure), P_{th} and E_{th} are, respectively, the thermal pressure and energy including the ideal-gas contribution plus that of lattice vibrations. The most commonly used expressions for the Grüneisen parameter γ_G, namely, the Slater ($m=0$), Dugdale-McDonald ($m=1$), and
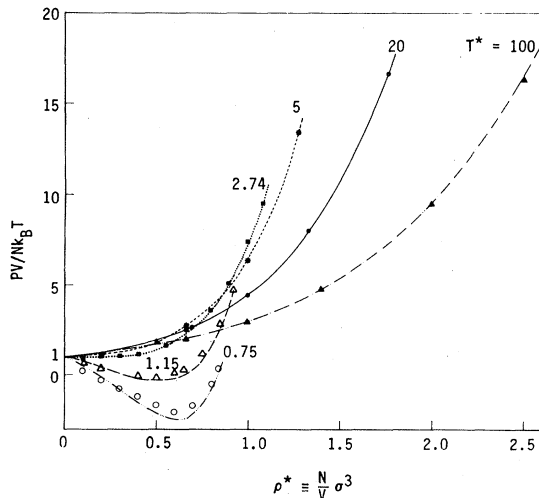
FIG. 2. Compressibility factor PV/Nk_BT as function of reduced density and reduced temperature for the Lennard-Jones fluid. See caption to Fig. 1.
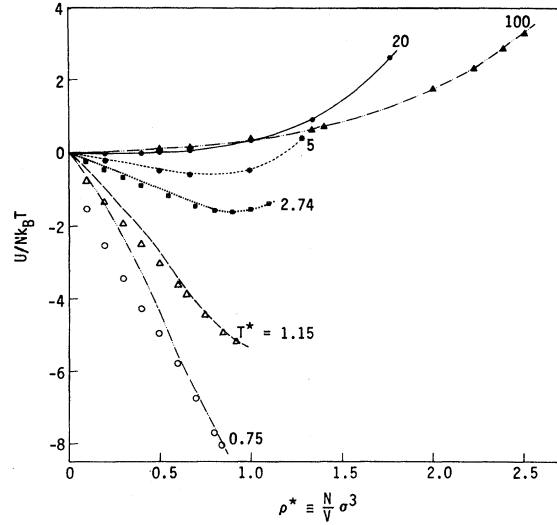
FIG. 3. Excess energy U/Nk_BT as function of reduced density and reduced temperature for the Lennard-Jones fluid. See caption to Fig. 1.

"free volume" ($m=2$) can be summarized by[21]

$$\gamma_G(\rho)=\tfrac{1}{2}\gamma_G^E(\rho)+\tfrac{1}{3} , \qquad (22)$$

with

$$\gamma_G^E(\rho)=\frac{\partial}{\partial\ln\rho}$$
$$\times\left[\ln\left|\rho^{2m/3}\frac{\partial}{\partial\rho}[P_0(\rho)\rho^{-2m/3}]\right|\right] . \qquad (23)$$

For a classical harmonic solid $E_{\text{th}}=3T$, so that the excess energy (without the ideal-gas contribution) is

$$E^E=U_0(\rho)+\tfrac{3}{2}T , \qquad (24)$$

and the excess pressure is given by

$$P^E=P_0(\rho)+\tfrac{3}{2}\gamma_G^E\rho T . \qquad (25)$$

Integrating Eqs. (25) and inserting in Eq. (24) we obtain

$$\frac{S^E}{Nk_B}=s$$
$$=\tfrac{3}{2}\ln T-\tfrac{3}{2}\int\gamma_G^E(\rho)d\ln\rho+C , \qquad (26)$$

$$U^{(s)}(\rho,s)=U_0(\rho)$$
$$+\tfrac{3}{2}\exp\left[\tfrac{2}{3}(s-C)\right.$$
$$\left.+\int\gamma_G^E(\rho)d\ln\rho\right] , \qquad (27)$$

where the integral over γ_G^E is indefinite and all in-

TABLE II. Compressibility factor $Z = PV/Nk_BT$, excess internal energy $u = U/Nk_BT$, and excess entropy $s = -S^E/Nk_B$, on the isotherms T^*=0.75 and 1.15 for the Lennard-Jones fluid. Columns 2–4[a]: exact Monte Carlo computations (Ref. 18). Columns 5–7: "additivity" approximation.

ρ	Z	u	s	Z_a	u_a	s_a
			T^*=0.75			
0.1	0.23	−1.53	0.73	0.53	−0.64	0.20
0.2	−0.29	−2.53	1.05	−0.10	−1.39	0.44
0.3	−0.78	−3.44	1.34	−0.84	−2.26	0.74
0.4	−1.20	−4.28	1.60	−1.61	−3.25	1.08
0.5	−1.69	−4.97	1.75	−2.24	−4.32	1.50
0.6	−2.05	−5.81	2.08	−2.51	−5.45	2.00
0.7	−1.71	−6.76	2.59	−2.15	−6.56	2.59
0.8	−0.53	−7.71	3.24	−0.81	−7.58	3.27
0.84	+ 0.37	−8.05	3.52	+ 0.10	−7.95	3.57
			T^*=1.15			
0.1	0.61	−0.75	0.37	0.77	−0.41	0.19
0.2	0.35	−1.35	0.62	0.46	−0.88	0.42
0.3	0.12	−1.95	0.90	0.11	−1.43	0.69
0.4	−0.09	−2.48	1.14	−0.20	−2.05	1.01
0.5	−0.13	−3.02	1.43	−0.37	−2.71	1.38
0.6	0.07	−3.60	1.82	−0.25	−3.39	1.81
0.65	0.31	−3.87	2.03	−0.02	−3.73	2.05
0.75	1.17	−4.46	2.57	−0.91	−4.35	2.59
0.85	2.86	−4.93	3.15	2.67	−4.87	3.19
0.92	4.72	−5.18	3.62	4.53	−5.13	3.65

[a]See Tables VI and VII in Verlet and Weis, Phys. Rev. A 5, 939 (1972).

tegration constants are absorbed in the universal constant C. With the standard expressions (23) we now get

$$U_G^{(s)}(\rho,s) = U_0(\rho)$$

$$+ \frac{3}{2}\left[\rho^{2m/3}\frac{\partial}{\partial\rho}[P_0(\rho)\rho^{-2m/3}]\right]$$

$$\times \exp[\tfrac{2}{3}(s - C)] . \tag{28}$$

Note that this expression is additive, i.e., if

$$U_0(\rho) = \sum_i \alpha_i U_{0,i}(\rho)$$

then

$$U_G^{(s)}(\rho,s) = \sum_i \alpha_i U_{G,i}^{(S)}(\rho,s) ,$$

and the standard Grüneisen theory obeys Eq. (9).

B. Generalized Grüneisen EOS

Using the idea of additivity of equations of state [Eq. (9)] and the inverse power potentials as a basis set, we may generalize the Grüneisen EOS by treating the inverse power solids in the harmonic approximation. A general expression for an harmonic inverse power solid is

$$s = -\frac{n}{2}\ln y_n + C^{(n)} , \tag{29}$$

where the constants $C^{(n)}$ depend on the specific mode of approximation (see below). If the zero isotherm is represented as a linear combination of inverse power-lattice sums,

$$U_0(\rho) = \sum_n \alpha_n(C_n\rho^{n/3})$$

then Eqs. (9) and (29) yield a generalized Grüneisen form

TABLE III. Compressibility factor $Z = PV/Nk_BT$, excess internal energy $u = U/Nk_BT$, and excess entropy $s = -s^E/Nk_B$, on the isotherms $T^* = 1.35$ and 2.74 for the Lennard-Jones fluid. Columns 2—4[a]: exact Monte Carlo computations (Ref. 18). Columns 5—7: additivity approximation.

ρ^*	Z	u	s	Z_a	u_a	s_a
			$T^* = 1.35$			
0.1	0.72	−0.58	0.29	0.83	−0.35	0.19
0.2	0.50	−1.12	0.56	0.61	−0.75	0.41
0.3	0.35	−1.55	0.75	0.37	−1.21	0.68
0.4	0.27	−2.04	1.04	0.18	−1.72	0.98
0.5	0.30	−2.50	1.34	0.12	−2.27	1.34
0.55	0.41	−2.74	1.52	0.19	−2.55	1.53
0.70	1.17	−3.47	2.18	0.98	−3.35	2.21
0.80	2.42	−3.89	2.70	2.25	−3.81	2.74
0.90	4.58	−4.19	3.28	4.38	−4.15	3.33
0.95	6.32	−4.23	3.56	5.82	−4.25	3.66
			$T^* = 2.74$			
0.1	0.97	−0.22	0.19	1.02	−0.16	0.17
0.2	0.99	−0.44	0.39	1.04	−0.34	0.37
0.3	1.04	−0.65	0.60	1.08	−0.54	0.59
0.4	1.20	−0.86	0.85	1.20	−0.76	0.85
0.55	1.65	−1.17	1.23	1.60	−1.09	1.30
0.70	2.64	−1.42	1.79	2.52	−1.38	1.82
0.80	3.60	−1.56	2.21	3.57	−1.51	2.22
0.90	5.14	−1.61	2.65	5.10	−1.57	2.67
1.00	7.39	−1.53	3.11	7.22	−1.52	3.15
1.08	9.58	−1.39	3.55	9.48	−1.38	3.57

[a]See Table VIII and IX in Verlet and Weis, Phys. Rev. A 5, 939 (1972).

$$s = \frac{3}{2}\ln T - \frac{3}{2}\ln\left[\sum_n \alpha_n \rho^{n/3}\exp(-\tfrac{2}{3}C^{(n)})\right],$$

$$(30)$$

$$U^{(s)}(\rho,s) = \sum_n \alpha_n (C_n \rho^{n/3})$$

$$+ \frac{3}{2}\left[\sum_n \alpha_n \rho^{n/3}\exp(-\tfrac{2}{3}C^{(n)})\right]$$

$$\times \exp(\tfrac{2}{3}s) .$$

$$(31)$$

The accuracy of these equations of state depends on the constants $C^{(n)}$. The standard expressions (23) employ

$$C^{(n)} = -\frac{3}{2}\ln\left[C_n\frac{n}{3}\left[\frac{n}{3}+1-\frac{2m}{3}\right]\right]+C ,$$

$$m = 0,1,2 . \quad (32)$$

Note that adding the same constant C to each $C^{(n)}$

does not affect $\gamma_G^E = (\partial \ln T/\partial \ln \rho)_s$, and Eqs. (30) and (31) remain the same provided we change s to $s + C$.

Other possiblities to determine the constants $C^{(n)}$ are considered below and the general validity of the additive EOS is demonstrated.

C. Lattice dynamics, Einstein approximation, and Debye-type models

The lattice dynamics (LD) calculations, in the harmonic approximation, consist of truncating a Taylor expansion of the lattice potential energy after the quadratic terms in the particle displacements. By changing to normal-mode coordinates the quasiharmonic Hamiltonian can be written as a sum of $3N - 3$ independent harmonic oscillator Hamiltonians. Denote by ν_i the frequency of the normal mode i $(\omega_i = 2\pi\nu_i)$, M is the mass of the particle, and let

$$\langle f(\nu)\rangle = \frac{1}{3N}\sum_{i=1}^{3N-3} f(\nu_i)$$

TABLE IV. Compressibility factor $Z = PV/Nk_BT$, excess internal energy $u = U/Nk_BT$, and excess entropy $S = -S^E/Nk_B$, on the isotherms $T^* = 5$, 20, and 100 for the Lennard-Jones fluid. Columns 2—4: "exact"[a] Monte Carlo computations (Ref. 18). Columns 5—7: additivity approximation.

ρ^*	Z	u	s	Z_a	u_a	S_a
			$T^*=5$			
0.2	1.169	−0.202	0.318	1.198	−0.157	0.333
0.5	1.867	−0.474	0.962	1.855	−0.424	0.987
0.666	2.628	−0.584	1.418	2.670	−0.535	1.442
1	6.336	−0.456	2.570	6.402	−0.415	2.586
1.279	13.44	0.435	3.796	13.31	0.420	3.800
			$T^*=20$			
0.2	1.270	−0.005	0.255	1.278	0.005	0.250
0.4	1.667	+ 0.009	0.531	1.682	0.025	0.539
0.666	2.508	0.083	0.982	2.527	0.100	0.987
1	4.458	0.348	1.656	4.471	0.362	1.676
1.333	7.999	0.942	2.499	8.039	0.968	2.509
1.765	16.68	2.65	3.822	16.62	2.64	3.829
			$T^*=100$			
0.2	1.221	0.036	0.173	1.225	0.038	0.173
0.5	1.675	0.115	0.468	1.685	1.121	0.462
1	2.95	0.361	1.029	2.97	0.369	1.039
1.4	4.76	0.734	1.580	4.75	0.736	1.594
2	9.50	1.767	2.590	9.51	1.775	2.599
2.222	12.10	2.346	3.036	12.17	2.375	3.028
2.38	14.46	2.887	3.336	14.47	2.896	3.352
2.5	16.29	3.304	3.620	16.45	3.348	3.611

[a]See Table IV in Hansen's paper (Ref. 18).

for any function of the frequencies. In particular, define the Einstein frequency v_E by

$$v_E^2 = \langle v^2 \rangle .$$ (33)

The excess entropy per particle in the LD harmonic approximations is[1,17]

$$\left[\frac{S^E}{Nk_B} \right]_{\text{LD}} = s_{\text{LD}} = s_{\text{Einstein}} + \Delta ,$$ (34)

where

$$s_{\text{Einstein}} = \frac{3}{2} \ln T - \frac{3}{2} \ln \frac{M\omega_E^2}{\rho^{2/3}} + C ,$$ (35)

with $C = \frac{3}{2} \ln 2\pi + \frac{1}{2}$, is the result of the Einstein approximation, and the "correction" is

$$\Delta = 3 \left\langle \ln \left[\frac{\omega_E}{\omega} \right] \right\rangle .$$ (36)

In the Einstein approximation for the frequency distribution,

$$\langle f(v^2) \rangle_{\text{Einstein}} = f(v_E^2)$$ (37)

for any function f.

For the inverse power potentials,

$$\frac{M\omega_E^2}{\rho^{2/3}} = \frac{2}{3} n (n - 1) C_{n+2} \rho^{n/3} \equiv 2\gamma_0^{2/3} D_n \rho^{n/3} ,$$

where D_n is the force constant. Lattice dynamics calculations[17] provide the "corrections" Δ_n. The constants $C^{(n)}$ from the LD and Einstein approximation are given by

$$C^{(n)}_{\text{Einstein}} = C - \ln 2 - \frac{3}{2} \ln D_n ,$$

$C^{(n)}_{\text{LD}} = C^{(n)}_{\text{Einstein}} + \Delta_n$, and numerical values for fcc solids are presented in Table I.

Consider the case when the pair potential is a linear combination of inverse powers, $\phi(r) = \epsilon \sum_n \alpha_n (\sigma/r)^n$. For every normal mode i we have $v_i^2 = \sum_n \alpha_n v_i^{(n)2}$ and in particular

$v_E^2 = \sum_n \alpha_n v_E^{(n)2}$. Within LD in the harmonic approximation, the additive EOS, i.e., Eqs. (30) and (31), is equivalent to the additional requirement

$$e^{\langle \ln v^2 \rangle} = \sum_n \alpha_n e^{\langle \ln v^{(n)2} \rangle} . \tag{38}$$

The equality (38) is, of course, satisfied by the Einstein approximation and we expect it to be accurate in general. For the LJ system near the triple-point-density, namely, $1/\rho^* = 0.972$, 0.997, 1.032, exact LD calculations[1] give $\gamma_G = 3.10$, 3.18, 3.30, respectively, while from Eqs. (30) and (31), with $C_{LD}^{(n)}$ we obtain 3.08, 3.15, and 3.26 as a demonstration of the accuracy of the additive EOS within LD. Just for comparison, the corresponding results with $C_{Einstein}^{(n)}$ are 3.17, 3.26, and 3.39.

Consider normalized frequency distribution of the type

$$G(v) = \begin{cases} \dfrac{g(v)}{F(v_{max})}, & v \leq v_{max} \\ 0, & v > v_{max} \end{cases}$$

where $F(v) = \int_0^v g(v)dv$, $\lim_{v \to 0}[f(v)\ln v] = 0$, and v_{max} is a characteristic Debye-type frequency obeying $v_{max}^2 = \sum_n \alpha_n v_{max}^{(n)2}$. Equation (38), i.e., additivity of EOS within LD, is exact provided

$$\frac{1}{F(v_{max})} \int_0^{v_{max}} F(v)\frac{dv}{v} = \text{const} .$$

That is the case for $g(v) = v^q (q \geq 0)$ where "const" $= 1/(1+q)$ and in particular for the Debye model $q = 2$.

A study of the frequency distribution, for different potentials in order to identify those particular features that lead to the general validity of Eq. (38), is currently underway. In general, the scaled spectrum $G(v/\bar{v})$, where $\bar{v}$ is some characteristic Debye-type frequency, plays a role similar to that of the pair function for fluids. Just as the universality of the pair functions, $g(r\rho^{1/3};s)$, the universality of the scaled spectrum, $G(v/\bar{v})$, will lead to additivity [i.e., Eq. (38)].

D. Computer simulations: the LJ system as a benchmark example

The computer-simulation data for the inverse power potentials ($n \leq 12$) are well satisfied by an expression of the form of Eq. (29) and in order to minimize the relative errors in the total pressure and excess entropy we determine the constants

$C_{MC}^{(n)}$ from the Monte Carlo data at the melting density: $C_{MC}^{(n)} = s_S + n/2 \ln y_n(s_S)$. From Table I we find that the difference $C_{LD}^{(n)} - C_{MC}^{(n)}$ remains practically the same (~ 0.08) for $n \leq 9$ and only for steeper potentials it becomes larger (i.e., ~ 0.20 for $n = 12$). This difference will manifest itself in the calculated γ_G^E for the LJ system. For the LJ system, the generalized Grüneisen EOS [Eqs. (30) and (31)] as obtained from "additivity" yields

$$\gamma_G^E = 4 + \frac{2}{A_{LJ}\rho^2 - 1} , \tag{39}$$

where

$$A_{LT} = \exp[\tfrac{2}{3}(C^{(6)} - C^{(12)})] . \tag{40}$$

Numerically, we get $A_{LJ} = 1.399$, 1.559, 1.847, 2.072, 2.211, and 2.493 for $m = 0,1,2$, [Eq. (23)], the Einstein approximation, LD, and MC values for $C^{(n)}$, respectively. The MC data for the LJ system[18] feature only 10% deviations from harmonicity near the melting transition for $T^* \leq 3$, i.e., for low solid densities: $U_{th}^E \simeq 1.35$ T vs 1.5 T for an harmonic solid. Defining $\gamma_G^E = P_{th}^E/\rho U_{th}^E$ and using the representation (39) to obtain A_{LJ} from the MC data, we find that, to within about 2%, $A_{LJ}^{MC} = 2.35$ for all densities for which MC data is available. This value for A_{LJ} falls midway between the results (40) with $C_{LD}^{(n)}$ and $C_{MC}^{(n)}$. Considering the above 10% deviations from harmonicity, our predictions for the pressure should be compared via $A \simeq 2.35(1.5/1.35) = 2.61$, which is much closer to the result (40) with $C_{MC}^{(n)}$ than that with $C_{LD}^{(n)}$. Thus the additive EOS with the $C_{MC}^{(n)}$ predicts the MC results for the total pressure of LJ solid to better than 1%. The 10% error in the harmonic prediction for U_{th}^E decreases with increasing density, and anyway is equivalent to about 1% error for the *total* excess energy. Finally, the accuracy of the additive EOS is also exhibited when considering the excess entropies; e.g., for $T^* = 1.35$ and $\rho^* = 1.05$ (near melting) the MC result is $s = -4.913$ and from Eq. (30) with $C_{MC}^{(n)}$ we get $s = -4.892$. The overall accuracy of Eqs. (30) and (31) with $C_{MC}^{(n)}$ is about 1% for the LJ solid, within the statistical error of the MC data.

VI. MELTING TRANSITION: ADDITIVITY OF MELTING CURVES

The accurate EOS obtained from Eq. (11) for both the fluid and solid phases, especially near the melting transition, ensures good predictions for the

melting characteristics through Eqs. (14). Instead of an exact numerical solution for the LJ system, we find it more instructive to analyze the predictions of Eq. (11) in order to find an approximate solution that is both accurate and general.

First observe that the MC results (Table I) for the melting characteristics of the relatively soft ($n \leq 12$) inverse power potentials reveal that $s_L^{(n)}$ and $s_S^{(n)}$ are nearly n independent, and that

$$1 < \frac{y_n(s_S^{(n)})}{y_n(s_L^{(n)})} < 1.04 \; .$$

Note that any separate "component" n in Eqs. (14) satisfies these equations provided we take the particular $s_L^{(n)}$ and $s_S^{(n)}$ and maintain

$$\frac{\rho_s^*}{\rho_L^*} = \frac{y_n(s_S^{(n)})}{y_n(s_L^{(n)})} \equiv \delta_n \; .$$

Let n_0 be the largest n appearing in Eqs. (14), i.e., $n_0 = 12$ for the LJ system. The exact large-T^* limit solution for Eqs. (14) is given by $\rho_S^*/\rho_L^* = c\delta_{n_0}$ and $s_L = s_L^{(n_0)}, s_S = s_S^{(n_0)}$ while c is to be determined from Eq. (12). However, in view of the above two features of the inverse power-melting transition, this asymptotic large-T^* solution will satisfy Eqs. (14) for each n separately to about 2%, and the closer n is to n_0 the better is the "n_0 solution" for the particular component n. Detailed inspection of the n_0 solution reveals that it is an excellent first-order solution of Eqs. (14) and (12) for any value of T^*: Near the melting transition for any inverse power potential the relative error in the value of y_n is related to the error in s by $\delta y_n/y_n \sim 2/n \delta s$. Deviations among the $s_L^{(n)}$'s and $s_S^{(n)}$'s are in order of 0.1 making the relative shift $\delta y_n/y_n$ of order (or less than) 5%, but the resultant changes are similar on both sides of Eqs. (14) and cancel.

An approximate description of the melting temperature and pressure, along the fluid and solid sides of the transition of accuracy comparable with the n_0 solution described above, is obtained by taking for each component n on the right- (left-) hand side of Eqs. (14), the value s_L (or s_S) corresponding to the value appropriate for the transition for that particular inverse nth power potential, i.e., $s_L = s_L^{(n)}(s_S = s_S^{(n)})$. This approximate solution, which would have been the exact solution of Eqs. (14) if s_L and s_S were universal constants, describes "additivity of melting curves," since the liquidus (L) and solidus (S) are features as lines of constant excess entropies. Let $\phi(r) = \sum_i \alpha_i \phi_i(r)$ be a linear combination of potentials ϕ_i for which $T_M^{(i)}(\rho_S)$,

$P_M^{(i)}(\rho_S)$ describes the melting temperature and pressure as functions of the melting density. Additivity of melting curves predicts that the melting temperature and pressure, $T_M(\rho_S), P_M(\rho_S)$, for the potential ϕ are given by

$$T_M(\rho_s) = \sum_i \alpha_i T_M^{(i)}(\rho_S) \; , \tag{41}$$

$$P_M(\rho_S) = \sum_i \alpha_M^{(i)}(\rho_S) \; , \tag{42}$$

and two similar equations hold also for ρ_L. A measure of the accuracy of this description is provided by the discrepancy between the functions $P_M(T_M)$ as obtained from the ρ_L and ρ_S melting equations. The triple point is characterized by $P_M \cong 0$.

The concept of additivity of melting curves has been derived[22,23] some years ago by approaches closely related to the one employed here and its accuracy as demonstrated by many examples provides an additional check on the validity of the additive EOS. As a matter of fact, the concept of additivity of melting curves proved to be more accurate than could have been expected on the basis of these earlier deviations, while its accuracy is compatible with our analysis based on the additive EOS.

A consistency check for the LJ system can be constructed as follows. Additivity of melting curves yields

$$T_M^* = 4 \left[\left[\frac{\rho_S^*}{0.844\sqrt{2}} \right]^4 - \left[\frac{\rho_S^*}{1.56\sqrt{2}} \right]^2 \right]$$

along the melting line which is expected to be also a line nearly constant s (i.e., s_S). Thus we expect

$$\gamma_G^E = \frac{\partial \ln T_M}{\partial \ln \rho_S} = 4 + \frac{2}{A\rho^2 - 1}$$

with

$$A = \frac{1.56^2}{2 \times 0.844^2} = 2.398 \; .$$

This value for A is consistent with that obtained from the MC data.

The apparent validity of additivity of melting curves also in two dimensions[24] (2D), indicates that the additive EOS [i.e., Eq. (9)] holds in two dimensions (2D). Extension of the computer-simulation data[25] for the 2D LJ and soft-sphere (r^{-12} potential) system and the generation of similar data for the r^{-6} potential, could provide a benchmark test of Eq. (9) in two dimensions.

VII. SUMMARY AND CONCLUSIONS

Using the variational fitting procedure, we gave a new interpretation to a large number of published variational perturbation calculations, to find the universality of the fitting functions. It is expected that a single soft-core potential may provide, by a first-order variational calculation via the Gibbs-Bogoliubov inequality, the EOS for any other soft-core potential to an accuracy comparable with that of the simulations [the crucial step is to make the jump in fitting function space from $\delta S_0(\eta)=0$ for hard spheres, to $\delta S_0(\eta)=$ some universal function for soft spheres and other soft-core potentials]. The assumption of universality of the VFP fitting functions leads to additivity of equations of state when these are expressed in terms of the density and excess entropy as the independent variables. This offers a powerful tool in EOS calculations (similar to variational quantum-mechanical calculations): Knowing the EOS for a "basis set" of potentials and expanding (fitting) a given pair potential as a linear combination of functions (potentials) belonging to the basis set, a highly accurate EOS for the given potential can be obtained very easily. In fact, all the results presented in this work were obtained with a simple desk calculator. Two equally good fits of a given potential by different basis potentials should produce equally accurate equations of state, the discrepancies between which should give an idea about the quality of each. The first (fitting) stage of the calculation can be performed with any (experimental) data for the given potential (material)

which is expected to be additive in (effective) pair-potential contributions and in particular the zero-temperature isotherm. A benchmark test of the accuracy of the statistical mechanical stage of the calculation is provided by the computer-simulation data for the r^{-12}, r^{-6}, and LJ potentials, with very encouraging results. Analysis of the EOS of simple classical solids in the harmonic approximation shows in a simple analytical manner how the approximation of additivity of equations of state improves upon standard theories. Finally, it was shown how the known melting characteristics for the inverse power potentials, together with an approximate solution of the solid-fluid equilibrium equations for the additivity model, give rise to a simple and accurate description of the melting characteristics for soft-core potentials in terms of those for inverse power potentials. There are favorable indications for the validity of the above new methods in two dimensions as well.[26]

Pending further analysis and tests, we may nevertheless conclude from the results of the present work that the method based on additivity of equations of state gives a new and powerful approach to equation-of-state calculations.

ACKNOWLEDGMENT

[1]A comparative study of various theories for simple classical solids is given by, e.g., A. C. Holt, W. G. Hoover, and D. R. Shortle, Physica **49**, 61 (1970).

[2]See, e.g., the extensive review article by J. A. Barker and D. Henderson, Rev. Mod. Phys. **48**, 587 (1976), and J. P. Hansen and I. R. McDonald, *Theory of Simple Liquids* (Academic, New York, 1976).

[3]G. I. Kerley, J. Chem. Phys. **73**, 469 (1980); **73**, 478 (1980); **73**, 487 (1980).

[4]Y. Rosenfeld, J. Chem. Phys. **73**, 5753 (1980); **73**, 5760 (1980).

[5]See, e.g., Ref. 2, Appendix A of Ref. 4, and G. A. Mansoori and F. B. Canfield, J. Chem. Phys. **51**, 4958 (1969).

[6]N. W. Ashcroft and D. Stroud, Solid State Phys. **33**, 1 (1978). See also, Y. Rosenfeld, Phys. Rev. A **15**, 2545

(1977), and references therein.

[7]N. F. Carnahan and K. E. Starling, J. Chem. Phys. **51**, 635 (1969).

[8]M. S. Wertheim, Phys. Rev. Lett. **10**, 321 (1963).

[9]M. Ross, Phys. Rev. A **8**, 1466 (1973).

[10]M. Ross and D. Seale, Phys. Rev. A **9**, 396 (1974).

[11]M. Ross, J. Chem. Phys. **71**, 1567 (1979).

[12]H. E. DeWitt, in *Strongly Coupled Plasmas*, edited by G. Kalman (Plenum, New York, 1978); H. E. DeWitt, Phys. Rev. A **14**, 1290 (1976).

[13]H. E. DeWitt and Y. Rosenfeld, Phys. Lett. **75A**, 79 (1979); A. Beram and Y. Rosenfeld, J. Phys. C **13**, L787 (1980); Y. Rosenfeld and A. Baram, J. Chem. Phys. **75**, 427 (1981).

[14]Y. Rosenfeld and N. W. Ashcroft, Phys. Rev. A **20**, 1208 (1979).

[15]J. P. Hansen, Phys. Rev. A **8**, 3096 (1973).

[16]W. G. Hoover, M. Ross, K. W. Johnson, D. Henderson, J. A. Barker, and B. C. Brown, J. Chem. Phys. **52**, 4931 (1970).

[17]W. G. Hoover, S. G. Gray, and K. E. Johnson, J. Chem. Phys. **55**, 1128 (1971).

[18]J. P. Hansen, Phys. Rev. A **2**, 221 (1970); J. P. Hansen and L. Verlet, Phys. Rev. **184**, 151 (1969). A recent analytic representation of thermodynamic data for the Lennard-Jones fluid is given by F. Ree, J. Chem. Phys. **73**, 5401 (1980), and see references therein.

[19]It is instructive to compare the results of our new method (essentially a zero-parameter fit) with those of the elaborate fits in Ref. 18.

[20]S. G. Brush, in *Progress in High Temperature Physics and Chemistry,* edited by C. A. Rouse (Pergamon, London, 1967), Vol. 1.

[21]L. V. Altshuler, Sov. Phys. Usp. Fiz. Nauk **85**, 197 (1965) [Sov. Phys. Usp. **8**, 52 (1965)]; V. N. Zharkov and V. A. Kalinin, *Equations of State for Solids at High Pressures and Temperatures,* translated from Russian (Consultants Bureau, New York, 1971).

[22]Y. Rosenfeld, Mol. Phys. **32**, 963 (1976).

[23]Y. Rosenfeld, and R. Thieberger, Phys. Rev. A **15**, 1269 (1977).

[24]Y. Rosenfeld, Phys. Rev. A **24**, 2805 (1981).

[25]S. Toxvaerd, J. Chem. Phys. **69**, 4750 (1978); F. vanSwol, L. Woodcock, and J. N. Cape, J. Chem. Phys. **73**, 913 (1980); J. A. Barker, D. Henderson and F. F. Abraham, Physica **106A**, 226 (1981).

[26]Y. Rosenfeld, J. Phys. C (in press).